ACI MATERIALS JOURNAL TECHNICAL PAPER

Title no. 107-M63

Corrosion Process of Steel Bar in Concrete in Full Lifetime

by Yingshu Yuan, Jianhua Jiang, and Tao Peng

The corrosion current density of steel bar in concrete is measured during a corrosion process under the conditions of constant climate and chloride attack. The corrosion process shows the characteristics of the time-variant corrosion rate, and the four phases in the corrosion process are presented. The effects of the concrete water-cement ratio (w/c) on the variation of corrosion current densities are discussed, which shows that the influences of the variation of the corrosion current density and the cracking time are obvious. The mechanism analyses of the time-variation characteristics are carried out based on the microstructure of the interfacial transition zone (ITZ) between the steel bars and the concrete at different corrosion levels. The growth of the corrosion layer and the corrosion cracking are the main factors influencing the corrosion process. Finally, the time-dependent model of the corrosion rate variation and the corresponding model of the corrosion loss accumulation are presented.

Keywords: chloride attack; corrosion rate; interfacial transition zone; time variation.

INTRODUCTION

Corrosion is a slow process in a natural climate environment; thus, building a model of corrosion rate in concrete is arduous work. Corrosion can be accelerated in an artificially controlled environment, and the time-variation characteristics in the corrosion process can be studied under a constant climate condition.

According to published information, numerous models for predicting the corrosion rate have been presented. One area that has gained the attention of researchers is the time dependence of the corrosion rate in concrete. The researches show the descending characteristics of the corrosion rate in the corrosion process.[1,2] Furthermore, they show the test results of corrosion current I_c versus time of exposure, and the I_c values increasing with time of exposure.[3] This indicates that the corrosion rate is a time-dependent variable.[4] Earlier studies have also presented a time-dependent model for reinforcement corrosion in concrete[5]; however, the process in the full lifetime and mechanism of the time-variant corrosion rate merits further study.

Some researchers have been interested in the time variation of corrosion loss. One study[5] proposed a more detailed phenomenological model for the corrosion of steel reinforcement as a function of time. Another study[6] presented the degree of the corrosion as a function of time based on testing measurements. The quantitative prediction of the time-dependent corrosion loss accumulation should also be studied further.

In this paper, the changes of the corrosion current density in test specimens are measured in full lifetime under an artificially controlled environmental condition. Three kinds of mixture proportions of concrete are designed in the test specimens. The mechanisms of the corrosion rate at different time-variant phases are discussed. Finally, the time-dependent models of corrosion rate and corrosion loss in full lifetime are presented.

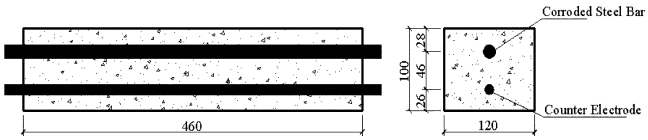

Fig. 1—Specimen design.

Table 1—Mixture proportions of concrete, 2400 kg/m^3 (4045.3 lb/yd^3)

Concrete grade	*w/c*	Cement, kg (lb)	Water, kg (lb)	Sand, kg (lb)	Aggregate, kg (lb)
C20	0.62	342.37 (754.78)	212.27 (467.97)	712.12 (1569.93)	1133.24 (2498.32)
C25	0.54	393.44 (867.37)	212.46 (468.39)	629.51 (1387.81)	1164.59 (2567.44)
C30	0.48	441.99 (974.40)	212.15 (467.70)	579.01 (1276.48)	1166.85 (2572.42)

RESEARCH SIGNIFICANCE

Studies on the changes of corrosion rate in full service life carried out under a constant climate condition effectively reveal the time-variant effect. Predicting the service life of a concrete structure in a natural climate and chloride attack environment is complicated work. Thus, building time-dependent models of corrosion rate and corrosion loss in full lifetime under a constant climate condition is essential research work. These research works will be beneficial in building prediction models of corrosion rate in a natural climate environment.

MEASUREMENTS OF CORROSION RATE

Corrosion potential and corrosion current density are measured in the full corrosion process under a constant climate environmental condition to study the characteristics of the time-variant corrosion rate.

Specimens

The specimen design is shown in Fig. 1. Three grades of concrete strength were designed, and their mixture proportions are presented in Table 1. The specimens were divided into three groups, which are summarized in Table 2. NaCl of 4% cement weight was mixed into the concrete to accelerate steel bar corrosion.

The specimens were cured for 28 days under standard curing conditions. After curing, the specimens and a reference specimen were dried until the relative humidity (RH) in the

ACI Materials Journal, V. 107, No. 6, November-December 2010.
MS No. M-2009-210.R4 received March 14, 2010, and reviewed under Institute publication policies. Pertinent discussion including authors' closure, if any, will be published in the September-October 2011 *ACI Materials Journal* if the discussion is received by June 1, 2011.

Yingshu Yuan *is a Professor of civil engineering at China University of Mining and Technology, Beijing, People's Republic of China. His research interests include durability test methods, concrete durability, and durability assessment of concrete structures in service.*

Jianhua Jiang *is a PhD Student at China University of Mining and Technology.*

Tao Peng *is a Graduate Student at China University of Mining and Technology.*

Table 2—Specimen grouping

Specimen mark	Steel bar		Concrete cover thickness, mm (in.)	Concrete grade
	Type	*d*, mm (in.)		
SR-A	HRB335	16 (0.630)	20 (0.787)	C20
SR-B				C25
SR-C				C30

concrete dropped to approximately 90%. The temperature and RH of the reference specimen were measured using a sensor probe. The specimens were then moved into an artificially controlled climate environment, wherein the temperature and humidity were controlled at 30 ± 2°C (86 ± 4°F) and RH 85 ± 5%, respectively.

The corrosion rates of the specimens were measured at regular intervals in the artificially controlled climate environment. The tests were stopped when the crack width caused by corrosion achieved approximately 0.5 mm (0.02 in.).

The compression strengths of the three kinds of concrete were measured after curing. The compression strengths of C20, C25, and C30 concrete grade were 23.5, 27.8, and 34.3 MPa (3408.21, 4031.83, and 4974.53 psi), respectively.

Measuring corrosion rate

The corrosion current density was obtained using the electrochemical analysis system based on the linear polarization resistance method. According to the corrosion electrochemical principle, the corrosion rate is proportional to the corrosion current density. The time-variant process of the corrosion current density indicates the process of the corrosion rate. The setup for the measurement is shown in Fig. 2.

Time-variant process of corrosion rate

The measurements of the time-dependent corrosion current density are shown in Fig. 3 and 4. The variation process was divided into five phases during the measuring time. The first phase involved the steel bar in its initial corrosion stage; here, the corrosion current density gradually increased from zero. The corrosion current densities in this phase were not measured. The initial corrosion was in the concrete hardening stage, as NaCl was mixed into the concrete to accelerate the corrosion of the steel bar. In this paper, the measurements were carried out from the second phase.

Figures 3 and 4 reveal that a descending phase initially occurred. The rate of descent then slowed down. After the second phase (TP-2), the rate remained steady in the third phase (TP-3). Afterwards, the concrete cover cracked due to corrosion expansion, and the rate gradually ascended in the fourth phase (TP-4). Throughout the fourth phase, the development of the rate entered another steady phase (TP-5).

MECHANISM ANALYSES OF TIME-VARIANT CORROSION RATE

Corrosion layer

The interfactial transition zone (ITZ) between the uncorroded steel bars and concrete is a porous zone, and

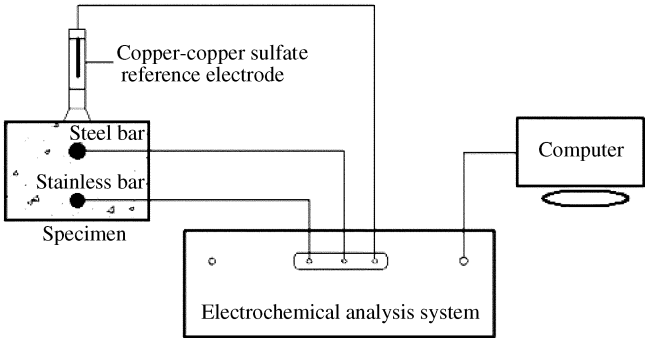

Fig. 2—Testing setup.

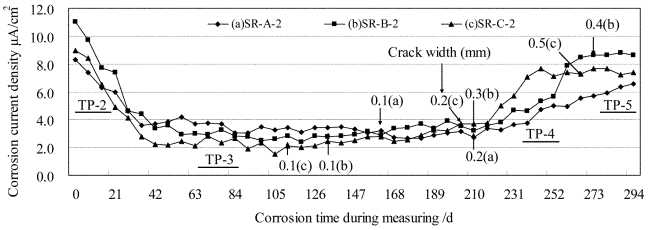

Fig. 3—Time-variant process of corrosion current density (1). (Note: 1 mm = 0.0394 in.)

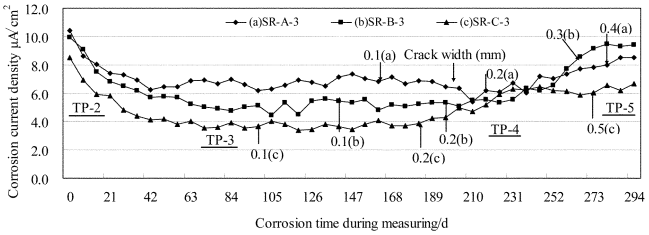

Fig. 4—Time-variant process of corrosion current density (2). (Note: 1 mm = 0.0394 in.)

this characteristic provides space for the diffusion of corrosion products. Reference 7 indicates that corrosion products propagate to the ITZ due to the expansion of the corrosion products, and the porous ITZ gradually transforms into a dense corrosion product layer, which is simply called a corrosion layer.

A digital optical microscope was used for observing the distribution of the corrosion layer along the perimeter of the steel bar. The observed samples were cut from the specimen at the different corrosion phases, as shown in Fig. 1. Before cutting, the specimen with a large crack width was fixed along the perimeter of the specimen by a piece of gauze soaked with epoxy.

The microscope measures the thickness of the corrosion layer depending on the variation in the color and in the microstructure (Fig. 5). It is an approximate measurement, but it is enough for determining the pattern of the distribution.

The interface along the perimeter of the steel bar was divided into 12 regions for measurement. The measurement arrangements are shown in Fig. 6.

Growth of corrosion layer

According to Reference 8, the corrosion products are only distributed on the upper-half circumference of the steel bar facing the concrete cover. Therefore, the discussion

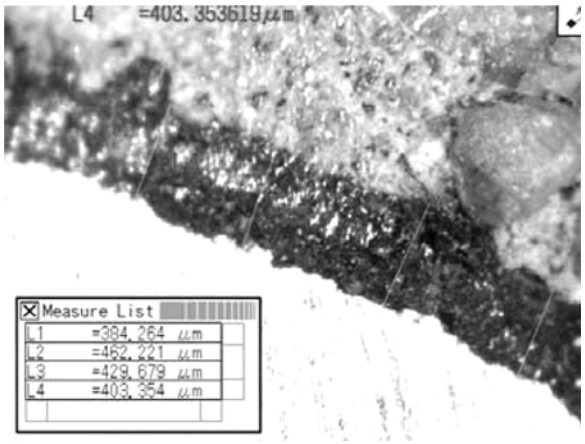

Fig. 5—Thickness of corrosion layer. (Note: 1 μm = 39.37 × 10^{-6} in.)

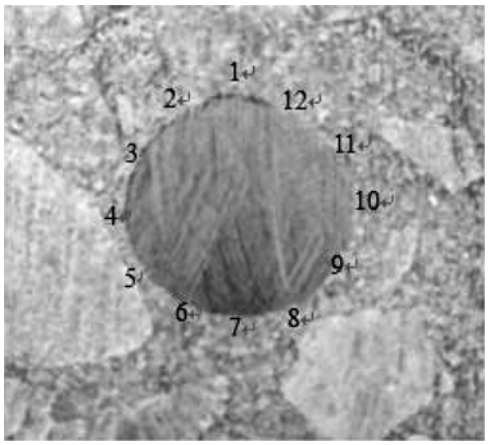

Fig. 6—Regional arrangements along circumference.

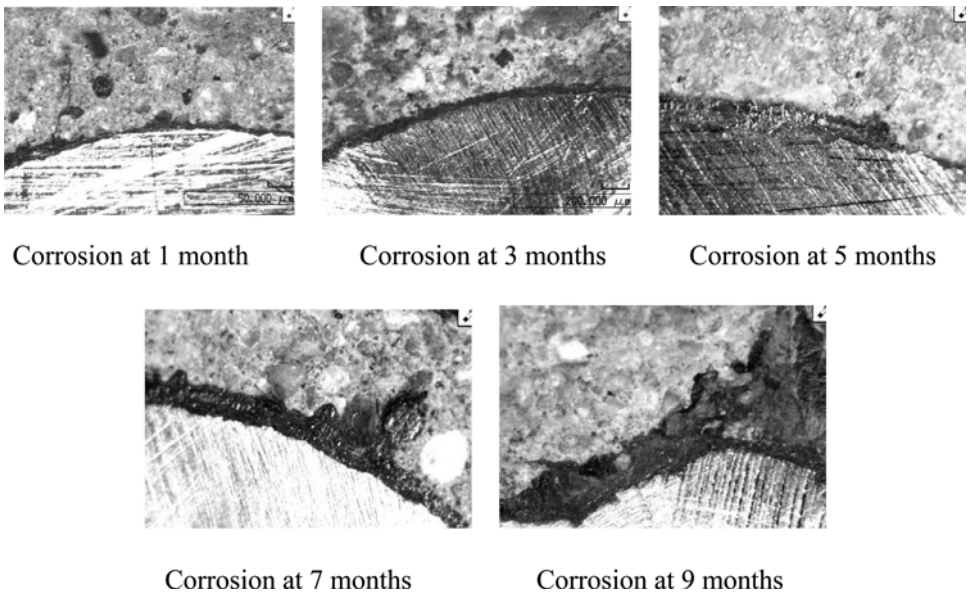

Fig. 7—Growth of corrosion layer at different corrosion phases (Specimen SR-A-2, H50).

regarding the growth of the corrosion layer is focused on the regions close to the concrete cover. Figures 7 and 8 show the growth of the corrosion layer in the corrosion process.

Mechanisms of time-variant process phases

Based on the growth of the corrosion layer, the mechanisms of the time-variant process phases are presented as follows:

1. Phase TP-2: The access of air is hindered as the porous ITZ gradually transforms into a dense corrosion layer. The rate of oxygen and moisture supply is reduced. Therefore, the anode reaction is inhibited, and the corrosion current density goes down.

2. Phase TP-3: When the corrosion current density decreases to a certain level, the equilibrium between the rates of consuming and transporting oxygen and moisture will be built, and the corrosion rate tends to become steady.

3. Phase TP-4: The concrete cover cracks. The cracking originates from the interface between the bar and the concrete, and it then passes through the concrete cover. The crack forms a new access for the infusion of oxygen and moisture. The rate of transporting oxygen and moisture is faster than the rate of consuming oxygen and moisture; thus, the corrosion rate tends to increase. The increase is very slow, however, at the initial cracking stage.

4. Phase TP-5: The corrosion products gradually fill up the cracks, and the access for the transportation of oxygen will be hindered again. After Phase TP-4 of the ascending phase, the corrosion rate will stop increasing and become steady. The conditions of the infusion of oxygen and moisture are similar to those in Phase TP-3.

Effect of concrete water-cement ratio (*w/c*) on growth of corrosion layer

Three concrete *w/c* are designed corresponding to three grades of concrete strength in the specimens. The *w/c* is a main factor influencing the porosity of the ITZ; its low ratio can result in dense concrete and dense ITZ. Figures 9(a) and (b) show the comparisons between the three corrosion layers, denoted as SR-A-3, SR-B-3, and SR-C-3 at 3 and 5 months of corrosion time, respectively. Corrosion Layer SR-A is thicker than Corrosion Layer SR-C, which means that the ITZ of Corrosion Layer SR-A is more porous. The rust

amount required for filling the ITZ at the initial phase in Corrosion Layer SR-A is higher than that in Corrosion Layer SR-C. The rust filling the ITZ at the initial phase is called the free expansion stage in Reference 9. Therefore, the development of the expansive force in Corrosion Layer SR-C is faster than that in Corrosion Layer SR-A, and the time of the concrete cover cracks in Corrosion Layer SR-C is earlier than that in Corrosion Layer SR-A based on the initial corrosion at the same time and under the same climate environmental condition.

Effect of concrete *w/c* on corrosion rate and process

Figures 3 and 4 also show the times when the concrete cover cracked based on a 0.1 mm (0.003937 in.) crack width on the specimens, and the times when the different levels of the crack width were achieved. Based on the comparison between Specimens SR-A-2 (C20) and SR-C-2 (C30) in Fig. 3, the corrosion current density of Corrosion Layer SR-A is higher than that of Corrosion Layer SR-C in Phase TP2 and TP3. The cracking time of Corrosion Layer SR-C, however, is earlier than that of Corrosion Layer SR-A based on the initial corrosion at the same time. After Phase TP3, the corrosion current density of Corrosion Layer SR-A is lower than that of Corrosion Layer SR-C. The comparisons indicate the effects of the concrete *w/c* on the variation process of the corrosion current density and corrosion cracking.

MODELING CORROSION PROCESS IN FULL LIFETIME

Corrosion loss accumulation based on corrosion current density

Corrosion loss accumulation ΔM is calculated based on the measured corrosion current density

$$\Delta M = \frac{N \times S \times \int i_{corr} \times t}{F} \quad (1)$$

where N is the gram-equivalent weight of the steel bar ($N = M/n$); F is the Faraday constant ($1F = 96{,}500C$/mol = 26.8 $A \cdot h$/mol); t is corrosion time; S is the total surface area of the steel bar in concrete, cm^2; and i_{corr} is the corrosion current density $i_{corr} = I/S(A/cm^2)$ [$A/in.^2$].

The average corrosion level ρ of the steel bar based on the corrosion amount ΔM is determined by Eq. (2)

$$\rho = \frac{\Delta M}{M_0} = \frac{N \times S \times \int i_{corr} \times t}{F \times M_0} \quad (2)$$

where M_0 is the original weight of the steel bar, g; and ΔM is the corrosion loss weight, g.

Measurements of actual corrosion loss weight of steel bar

After the measurements of the corrosion current were completed, the specimen was broken, and the corroded bar was cleaned using diluted hydrochloric acid. The weight of the cleaned bar was measured, and the actual corrosion loss weight and the corrosion level were determined by Eq. (3)

$$\rho = \frac{M_0 - M_1}{M_0} \times 100\% \quad (3)$$

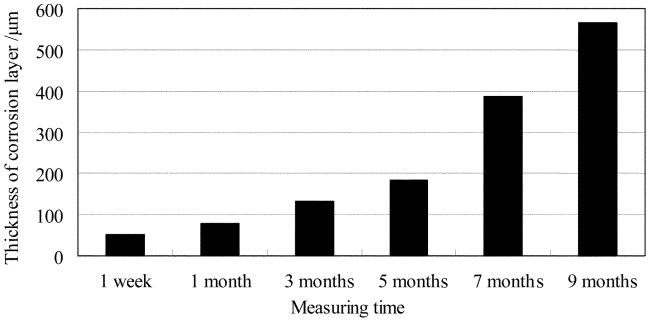

Fig. 8—Thickness development of Corrosion Layer SR-A-2. (Note: 1 μm = 39.37 × 10^{-6} in.)

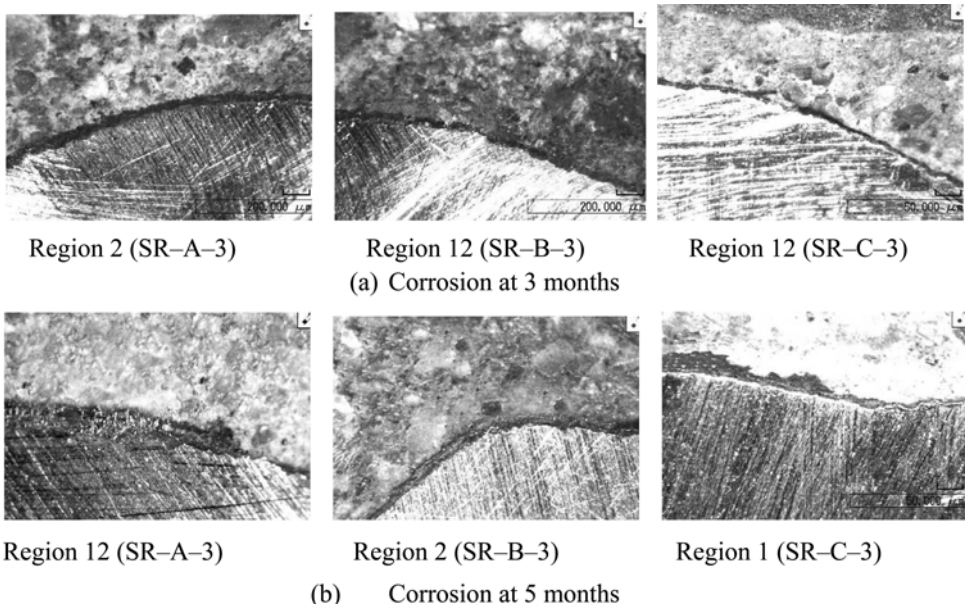

Fig. 9—Comparisons of Corrosion Layers SR-A-3, SR-B-3, and SR-C-3 at; (a) 3 months; and (b) 5 months.

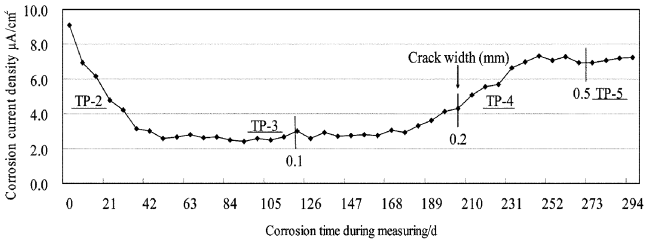

[1μA/cm^2 = 6.45μA/in.^{2}]

(a) Variation process of the corrosion current density (SR-C-2)

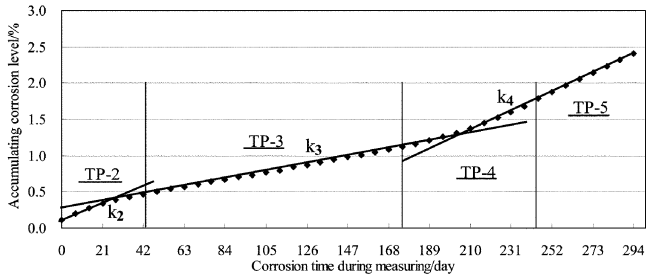

(b) Development of the average corrosion level (SR-C-2)

Fig. 10—Average corrosion level and corrosion rate at process phases.

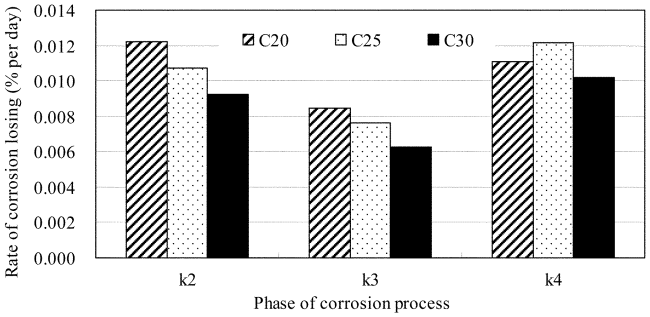

Fig. 11—Effects of concrete grades on corrosion rate.

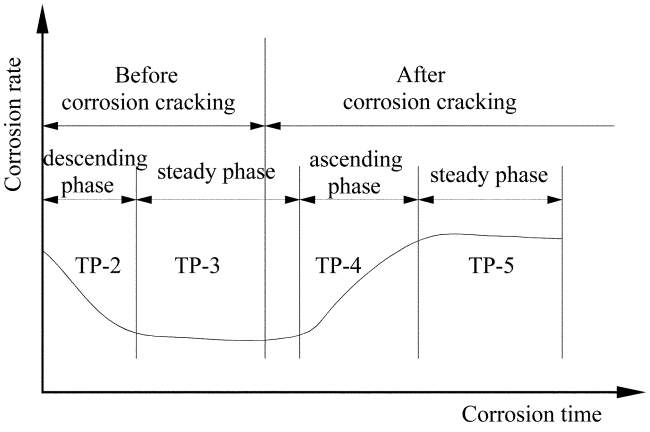

Fig. 12—Pattern model for time-variant process.

where M_1 is the weight of the cleaned steel bar, g.

Table 3 shows the comparison between the corrosion loss accumulation based on the corrosion current density and the actual corrosion loss weight.

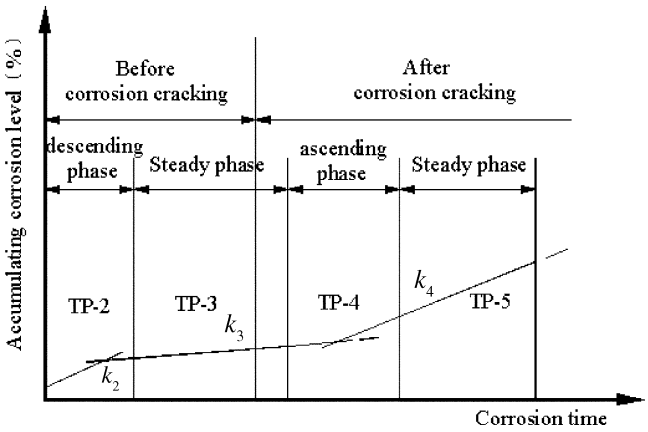

Fig. 13—Pattern model for corrosion rate at process phases.

Table 3—Comparison of corrosion level between calculated and weighed value

Specimen	Original weight M_0, g (lb)	Cleaned weight M_1, g (lb)	Calculated, ρ, %	Weighed, ρ, %
SR-A-2	697.5 (1.538)	676.1 (1.491)	3.1	2.8
SR-A-3	698.9 (1.541)	676.5 (1.491)	3.5	3.2
SR-B-2	694.8 (1.532)	678.4 (1.496)	2.4	2.2
SR-C-2	693.4 (1.529)	680.8 (1.500)	1.8	1.9

Modeling corrosion rate at process phases

The development of the average corrosion level indicates the corrosion loss accumulation. Figure 10(b) shows the development of the average corrosion level based on the variation process of corrosion current density shown in Fig. 10(a).

The corrosion rate can be simplified by constant values k_2, k_3, and k_4 shown in Fig. 10(b) from Phase TP-2 to TP-5. The comparison between Fig. 10(a) and (b) reveals the relationship between the rate of corrosion and the corresponding variation phase.

Figure 11 shows the effect of the concrete grade on the rate of corrosion loss.

Pattern models of variation process and corrosion rate

Figures 12 and 13 present the models for the time-variant process and the corrosion rate at the process phases based on the aforementioned tests and analyses.

CONCLUSIONS

1. A pattern model of the corrosion rate process in the full lifetime is established. The time-variant characteristics in the model are revealed. Under a constant climate environmental condition, the time-variant process of the corrosion rate in the full lifetime can be divided into five phases: a rising phase in the initial corrosion, a descending phase, a steady phase, an ascending phase, and another steady phase after the corrosion cracking. The discussions in this paper are from the second phase.

2. The mechanisms of the time-variant corrosion rate are discussed. The corrosion products propagate to the ITZ due to the expansion of the corrosion products, and the porous ITZ gradually transforms into a dense corrosion product layer. The growth of the corrosion layer at the ITZ is the main factor influencing the corrosion rate process.

3. The *w*/*c* is a main factor influencing the porosity of the ITZ. The microstructure at the ITZ in Specimen C20 shows more porous than at the ITZ in Specimen C30.

4. The corrosion loss accumulation in the full lifetime can be estimated based on the process of corrosion current density. The estimation method is presented. The corrosion rate can be simplified by constant values k_2, k_3, and k_4 from Phase TP-2 to TP-5.

5. The pattern model can be used to improve the existing prediction model. The accurate prediction model is an important part of predicting the service life of a reinforced concrete structure.

ACKNOWLEDGMENTS

The authors would like to express their appreciation to the National Science Foundation of China (NSFC). The research works belong to one part of Project No. 50878207 and 50538070, which are financially supported by the NSFC.

REFERENCES

1. Liu, T., and Weyers, R. W., "Modeling the Dynamic Corrosion Process in Chloride Contaminated Concrete Structures," *Cement and Concrete Research*, V. 28, No. 3, 1998, pp. 356-379.

2. Schiessl, P., and Raupach, M., "Laboratory Studies and Calculations on the Influence of Crack Width on Chloride-Induced Corrosion of Steel in Concrete," *ACI Materials Journal*, V. 94, No. 1, Jan.-Feb. 1997, pp. 56-62.

3. Baweja, D.; Roper, H.; and Sirivivatnanon, V., "Chloride-Induced Steel Corrosion in Concrete: Part 1—Corrosion Rates, Corrosion Activity, and Attack Areas," *ACI Materials Journal*, V. 95, No. 3, May-June 1998, pp. 207-217.

4. Vu, K.; Stewart, M. G.; and Mullard, J., "Corrosion-Induced Cracking: Experimental Data and Predictive Models," *ACI Structural Journal*, V. 102, No. 5, Sept.-Oct. 2005, pp. 719-726.

5. Mechers, R. E., and Li, C. Q., "Phenomenological Modeling of Reinforcement Corrosion in Marine Environment," *ACI Materials Journal*, V. 103, No. 1, Jan.-Feb. 2006, pp. 25-32.

6. Francois, R., and Arliguie, G., "Effect of Micro-Cracking and Cracking on the Development of Corrosion in Reinforced Concrete Members," *Magazine of Concrete Research*, V. 51, No. 2, Apr. 1999, pp. 143-150.

7. Yuan, Y. S.; Ji, Y. S.; and Jiang, J. H., "Effect of Corrosion Layer of Steel Bar in Concrete on Time-Variant Corrosion Rate," *Materials and Structures*, V. 42, No. 10, 2009, pp. 1443-1450.

8. Yuan, Y. S., and Ji, Y. S., "Modeling Corroded Section Configuration of Steel Bar in Concrete Structure," *Construction and Building Materials*, V. 23, No. 6, 2009, pp. 2461-2466.

9. Liu, Y. P., and Weyers, R. E., "Modeling the Time-to-Corrosion Cracking in Chloride Contaminated Reinforced Concrete Structures," *ACI Materials Journal*, V. 95, No. 6, Nov.-Dec. 1998, pp. 675-680.